ISSN 1392-2114 ULTRAGARSAS, Nr.2(30). 1998.

Theoretical and experimental investigation of dynamic characteristics of the cylindrical shell on a model

D. Gužas

Lithuanian Agricultural University

4324 Kaunas

Introduction

Many publications of different authors are devoted to the research of cylindrical shell vibration and sound insulation.

Most of the publications are of theoretical character. The obtained expressions are complicated and do not allow the character of dependence of the quantities under study upon the change of various parameters to be understood. This greatly reduces their value.

To determine the character of oscillations excitation, their propagation in the tube and impedance, special equipment was assembled. The report presents the methods of measurement performance as well the processing and analysis of the results obtained. Tube wall oscillations of the experimental equipment have been excited concentrically and parameters of propagated oscillations of the tube have been measured. It allowed the entrance impedance and admittance of the tube at narrow frequency bands to be defined.

In order to determine impedance and admittance by calculation method the computer program has been worked out.

The results obtained experimentally and theoretically are represented in diagrams. It is obvious from the diagrams that computed and experimental meanings of the entrance impedance model are in satisfactory agreement. Impedance meanings measured during the experiment are located slightly higher (are greater) than calculated ones.

Estimation of the power of vibration radiators

1.1. A problem of the field of a point-source radiator occurs frequently among the calculation schemes used for analysis of wave and vibrating processes. The case is that numerous constructions under real conditions or experimental situations get excited by forces distributed along very small areas and there is no possibility to specify these forces. A mathematical model in this case consists of the solution of the problem about the movement of a construction under the action of the concentrated force.

The most important characteristic defining the level excitation of a construction is the energy, radiated by field source per time unit, i.e., power of radiator *W*.

$W = F\dot{u}$.

Thus, if the calculation scheme is related to the assignment of the magnitude of force *F*, it is necessary for us to define the velocity of a construction at the point of fulcrum, i.e. $\dot{u}(t,0)$. For this purpose it is necessary to solve the corresponding problem of the dynamic theory of elasticity. In terms of frequency analysis this solution of a problem may be written with help of impedance $Z(-i\omega)$ in the form

$$\dot{u} = \frac{F}{Z(-iw)}.$$

And, consequently,

$$W = F^2|Z|^{-1}\cos\varphi$$

where $|Z|$ - modulus of impedance, and φ its argument.

It was this circumstance that defined the interest to the systematic accumulation of data on impedances of different thin-walled constructions.

1.2. These problems are reasonable in the case of function of the corresponding source having no special feature, more precisely, not turning into infiniteness (as, for example, at the concentrated excitation of the elastic semispace, etc.). It is impossible also not to see relation between the above-indicated dynamic problem and the traditional in theory elasticity problem of determining the rigidity coefficient [6]. Such coefficients of rigidity are determined easily from statistic problems for any bar constructions (e.g., shown in Fig. 1).

$$F = Cu, F = \frac{3EJ}{l^3}u, F = \frac{24}{5}\frac{EJ}{l^3}u, F = \frac{24EJ}{l^3}8u$$

where *E* - Young's modulus; *J* - inertia moment of cross-section; *l* - length of a bar. Or in the case of a circular plate, shown in Fig. 2a, or rectangular one, depicted in Fig. 2b.

S - area of the cross-section of a bar; ρ - material density.

If a shell is damped enough along its whole length, the useful estimate then is linked with the impedance of an infinite plate, which is being excited by the concentrated force [8].

$$Z = 8\sqrt{D\rho h} = 2.31\rho c h^2.$$

In case resonances manifest themselves in the shell, then instead of a formula for a semi-infinite bar at low frequencies it is necessary to apply the impedance of a

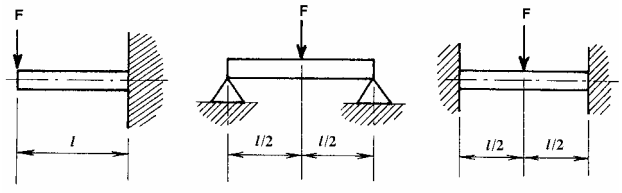

Fig. 1. **Scheme of impedance calculation of thin-walled bars a - console; b - supported span; c - fixed on the edges**

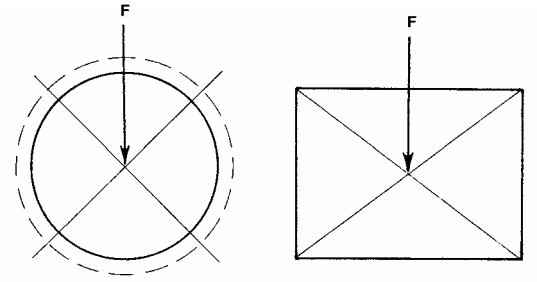

a) b)

Fig. 2. **Scheme of impedance calculation of thin-walled plates a - round; b - rectangular**

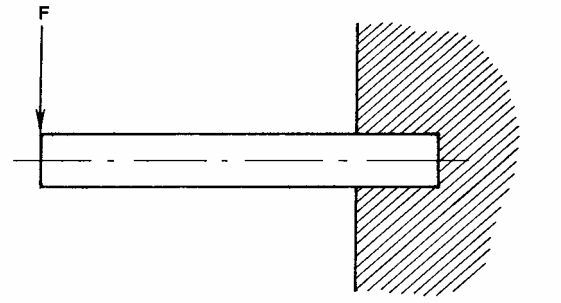

Fig. 3. **Scheme of impedance calculation of console damped material**

console

$$Z = \frac{EJk^3\left(1 + chkl\cos kl\right)}{\left(J_m klchkl - \cos klshkl\right)\left(-i\omega\right)}.$$

Finally, it is possible to study an exact expression for the impedance of a semi-infinite shell. Equations on this question as is shown in the work are written in the form (see Fig. 4).

$$\left.\begin{aligned} L_{11}u_1 + L_{12}u_2 + L_{13}u_3 &= 0 \\ L_{21}u_1 + L_{22}u_2 + L_{23}u_3 &= 0 \\ L_{31}u_1 + L_{32}u_2 + L_{33}u_3 &= \frac{p}{\rho hc^2} \end{aligned}\right\} \qquad (1)$$

$$C = \frac{16\pi D}{\left(3+\nu\right)} \cdot \frac{\left(1+\nu\right)}{R^2},$$

$$C = \pi^4 abD/4 \sum_n \sum_m \frac{1}{\left(\frac{m^2}{a^2} + \frac{n^2}{b^2}\right)^2}.$$

Thus it is possible to state that in the elasticity theory the extensive and still not duly systematised material on rigidity coefficients was accumulated, which allows one to approximately estimate impedances of constructions at low frequencies in the following way

$$Z\left(-i\omega\right) = C/\left(-i\omega\right).$$

where C - rigidity.

1.3. In the later period due to the development of dynamic positing of problems on the theory of rigidity in theory and practice of engineering calculations the notion of impedance, which was borrowed from the theory of electrical circuits, where energetic evaluations are of extreme importance, is frequently used [7]. Below we present methods of determination of impedances of thin-walled construction elements and indicate the spheres of their practical application.

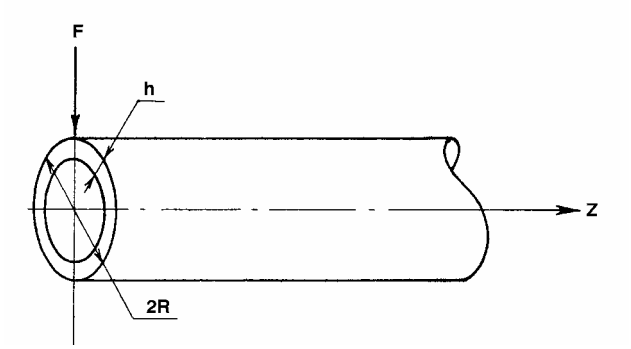

Fig. 4**. Scheme for impedance calculation of shell**

If in the damped shell at low frequency only a beam (flexural) wave, which corresponds to a normal wave with number *n=1*, gets excited, then useful for comparison should be the impedance of a semi-infinite bar (see Fig. 3).

$$Z = \frac{EJk^3\left(1+i\right)}{2}$$

where

$$k = \sqrt{\frac{\rho S\omega^2}{EJ}},$$

we come to the system of algebraic equations with a matrix of coefficients

$$b_{11} = \frac{\omega^2}{c^2} - \frac{1-\nu}{2R^2}n^2 - k^2, b_{12} = \frac{1-\nu}{2R}kn, b_{13} = -\frac{\nu ik}{R}$$

$$b_{21} = \frac{1+\nu}{2R}kn, b_{22} = \left(\frac{\omega^2}{c^2} - \frac{1-\nu}{2}\frac{n^2}{R^2}\right), b_{23} = -\frac{in}{R^2}$$

$$b_{31} = \frac{\nu ik}{R}, b_{32} = \frac{in}{R^2}, b_{33} = \left[\frac{\omega^2}{c^2} - \frac{1}{R^2} - \frac{h^2}{R^2}\left(k^2 + \frac{n^2}{R^2}\right)^2\right] \text{th}$$

us by Kramer's formula we find

$$V_{1n} = \frac{\Delta_{1n}}{\Delta_n}\frac{P}{4\pi^2 R}\frac{1}{\rho hc^2}, \quad V_{2n} = \frac{\Delta_{2n}}{\Delta_n}\frac{P}{4\pi^2 R}\frac{1}{\rho hc^2},$$

$$V_{3n} = \frac{\Delta_{3n}}{\Delta_n}\frac{P}{4\pi^2 R}\frac{1}{\rho hc^2} \qquad (2)$$

where Δ - the determinant of the system, and V_{3n} obtained Δ by substituting the third column by a column (0, 0, 1). From here we find

$$Z\left(-i\omega\right) = \frac{4\pi^2 R\rho hc^2}{\int_{-\infty}^{+\infty} \sum_{-\infty}^{+\infty} -n\frac{\Delta_{3n}}{\Delta_n} dk}\left(-i\omega\right). \qquad (3)$$

In the work [4] an expression of the normal impedance in a cylindrical shell is obtained. We shall obtain the expression for the normal impedance of the cylindrical shell in the form:

An expression for the concentrated force we expand according to Fourier

$$p = \frac{P}{R}\delta(\varphi)\delta(t) = \frac{P}{2\pi R}\left[\sum_{-\infty}^{+\infty} e^{in\varphi}\right]\left[\frac{1}{2\pi}\int_{-\infty}^{+\infty} e^{-izk}dk\right]$$

P - the magnitude of the concentrated force and applying the operators to Fourier series

$$u_3 = \int_{-\infty}^{+\infty}\sum_{-\infty}^{+\infty} V_{3n}e^{in\varphi}e^{-izk}dk$$

$$u_2 = \int_{-\infty}^{+\infty}\sum_{-\infty}^{+\infty} V_{2n}e^{in\varphi}e^{-izk}dk$$

$$u_1 = \int_{-\infty}^{+\infty}\sum_{-\infty}^{+\infty} V_{1n}e^{in\varphi}e^{-izk}dk$$

$$Z_n = -i\omega m \times \left[1 - \frac{\left(k^2 + \frac{n^2}{a^2}\right)^2}{k_u^4} - \frac{1}{k_n^2 a^2} - \right. \qquad (4)$$

$$\left. - \frac{\left(k^2 - k_t^2\right)\left(k^2 - k_n^2\right) - \frac{n^2}{a^2}k_n^2}{\left(k^2 + \frac{n^2}{a^2} + k_0^2\right)\left(k^2 + \frac{n^2}{a^2} - k_t^2\right)}\right]$$

When solving the problems on sound insulation of the cylindrical shell k is usually represented in the form $k = k_1 \sin\Theta_1 = k_2 \sin\Theta_2$ where $k_1 = \omega / c$ and $k_2 = \omega / c_2$ wave numbers in the media I and II inside and outside the shell, respectively, Θ_1 and Θ_2 the angles between the vectors k_1 and k_2 and the axis r. Considering these remarks, (4.27) can be rewritten in the form

$$Z_n = -i\omega m \times \left[1 - \frac{n^2}{f_k^2}\left(\sin^2\Theta + n^2\frac{f_c^2}{f^2}\right) - \right.$$

$$\left. - \frac{f_c^2}{f^2}\frac{\left(\sin^2\Theta - m_t^2\right)\left(\sin^2\Theta - m_n^2\right) - m_n^2\frac{n^2 f_c^2}{f^2}k_n^2}{f^2\left(\sin^2\Theta + n^2\frac{f_c^2}{f^2} - m_0^2\right)\left(\sin^2\Theta + \frac{n^2 f_c^2}{f^2} - m_t^2\right)}\right]. \qquad (5)$$

Here $m_t = c_c / c_t, m_n = c_c / c_n; m_0 = c_c / c_0, f_k = \frac{c_c^2}{2\pi}\sqrt{\frac{m}{B}}$ is the critical frequency at which the speed of flexural wave propagation is equal to the speed of wave propagation in the medium, B - flexural stiffness of the plate, from which the shell is formed, $f_n = c_n / 2\pi a$ the frequency at which one longitudinal wavelength in the bar will be equal to the circumference length of the shell $f_c = c_c / 2\pi a$ the frequency on which length of one sound wavelength in the medium will be equal to the circumference length of the shell, c_c and Θ the speed of wave propagation and the angle Θ in the first or the second medium.

Now let us analyse the expression obtained. First we shall consider the radial-symmetrical vibrations of the shell when *n=0*. Then

$$Z_n = -i\omega m\left[1 - \frac{f^2}{f_k^2}\left(\sin^4\Theta - \frac{f_n^2}{f^2}\frac{\sin^2\Theta - m_n^2}{\sin^2\Theta - m_0^2}\right)\right].$$

This is a well-known expression for the impedance of asymmetrical vibrations of the cylindrical shell. Attention is attracted to the fact that at low frequencies when $f_n > f$ the last member makes the main contribution. At the angle $\Theta_0 = \arcsin m_0$ becomes infinite ($Z_n = \infty$ in the absence of losses) and when $\Theta_n = \arcsin\Theta_n$ it is equal to zero. These angles are very close to each other since $c_n = c_0$. For a steel shell in the air Θ_n =3.8° while Θ_0 =3.7°. These angles have no appreciable effect on sound isolation, therefore the impedance may be considered as

$$Z_0 = -i\omega m\left[1 - \frac{f_0^2}{f_k^2}\sin^4\Theta - \frac{f_n^2}{f^2}\right].$$

At $f_n / f > 1$ the impedance increases when frequencies decrease and at $f \to 0, Z \to +i\infty$ i.e., the impedance becomes elastic. At the frequencies $f^2 >> f_n^2$

$$Z_0 = -i\omega m\left[1 - \frac{f^2}{f_k^2}\sin^2\Theta\right].$$

This is a well-known expression for the impedance of a plate. Now let us consider the value of the impedance of the shell for *n*>0. Here as well as at *n=0* the domains $f^2 << f_n^2$ and $f^2 >> f_n^2$ are distinguished. At $f^2 >> f_n^2$ the upper domain of frequencies is defined by the term $m_t^2 \cdot n^2 f_c^2 / f^2$. At small *n* when $\left(n^2 f_c^2 f_n^2 / f_\int^4\right) << 1$ the following term in (5) may be neglected. In this case the impedance is equal

$$Z_n = -i\omega m\left[1 - \frac{f^2}{f_k^2}\left(\sin^2\Theta + n^2\frac{f_c^2}{f^2}\right)\right].$$

Here we, too, neglect the influence of angles of coincidence along the longitudinal and shear waves which produce "splashes" Z_n at the angles $\Theta_0 = \arcsin\sqrt{m_0^2 - n^2 f_c^2 / f^2}$ and $\Theta_t = \arcsin\sqrt{m_t^2 - n^2 f_c^2 / f^2}$ since the range of angle variations is small and, besides, it may even become zero at sufficiently large.

At $f_n^2 >> f^2$ the expression for Z_n depends on the values of characteristic frequencies f_k and f_n. If $f_k > f_n$, then

$$Z_n = -i\omega m\left[1-\frac{f_n^2}{f^2}\frac{\left(\sin^2\Theta - m_t^2\right)\left(\sin^2\Theta - m_n^2\right) - m_n^2\frac{n^2 f_c^2}{f^2}}{\left(\sin^2\Theta + n^2\frac{f_c^2}{f^2} - m_0^2\right)\left(\sin^2\Theta + \frac{n^2 f_c^2}{f^2} - m_t^2\right)}\right].$$

It is possible to obtain the expression for Z_n in the case of sufficiently large angles Θ. At $\sin^2\Theta >> m_0^2$ and $\sin^2\Theta >> m_t^2$ obtain

$$Z_n = -i\omega m\times\left[1-\frac{f^2}{f_k^2}\left(\sin^2\Theta + n^2\frac{f_c^2}{f^2}\right) - \right.$$

$$\left. -\frac{f_n^2}{f^2}\frac{\sin^4\Theta}{\left(\sin^2\Theta + n^2\frac{f_c^2}{f^2}\right)^2} + n^2\frac{f_n^2 f_c^2 m_n^2}{f^4\left(\sin^2\Theta + n^2\frac{f_c^2}{f^2}\right)^2}\right]. \quad (7)$$

This expression holds true for all of the frequency range. It is possible to determine values Z_n in the domain of small angles Θ when $\sin^2\Theta >> m_t^2$. Then impedance

$$Z_n = -i\omega m\left[1 - n^4\frac{f_c^4}{f_k^2 f^2} - \frac{f_c^2}{f^2}\frac{m_t^2 + n^2\frac{f_c^2}{f^2}}{\left(n^2\frac{f_c^2}{f^2} - m_0^2\right)\left(n^2\frac{f_c^2}{f^2} - m_t^2\right)}\right] \quad (8)$$

It should be noted that the behaviour of Z_n with frequency is largely defined by the values of characteristic frequencies f_k and f_n since it lies below f_n (due to $c_n > c_c$).

At $f_n^2 >> f_k^2$ and $f > f_n$ the impedance quickly approaches the impedance of the plate (6). Quite a different character of the relation of $Z_n vs f$ is obtained when $f_k^2 >> f_n^2$ (a thick-walled shell of the small diameter). A case is possible when the value of the third term in (5) remains significant while the second term attains a significant influence. Then impedance Z_n will have an elastic character at almost all frequencies.

Up to the angles of coincidence on longitudinal and shear waves formula (8) may be used with high accuracy, and beyond these values, formula (7).

The present experiment, carried out on the special installation, gives the character of excitation and vibration propagation on the tube by concentrated excitation. The input impedance and admittance of the tube at narrow frequency bands has been defined too.

Methods of conducting measuring and data processing

Measuring of dynamic characteristics were conducted on an installation specially produced for this purpose (see Fig. 5). An installation consists of a steel tube (1) with a diameter s=0.72 m, wall thickness n=0.008 m (8 mm) and the total length 9 m. One end of the tube is suspended on a steel wire (2) to the stand (3) through bampers (4), as is

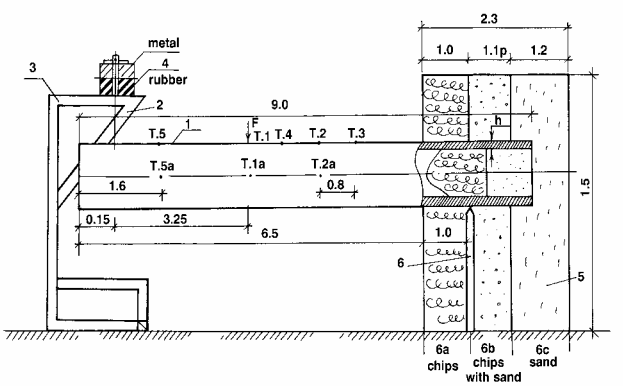

Fig. 5. **Experimental installation and location of measuring points on the tube**

shown in Fig.5. The other end is fixed to a special box (5), consisting of three sections, and rests on a metal support (6). In one section of the box (6a) the tube is damped with wood sawdust, in the other section (6b) with-dust and sand, and in the third section (6c) with pure sand. Inside the tube on the same end chips and sand may be also found. A free not damped and suspended end of the tube has a length of ~6.5m.

For carrying out measuring the apparatus of Brul and Kjear firm from Denmark were used. A model 8208 low hammer with an 8200-power generator was used as the source of vibration excitation. The hammer is made of three changeable strikers of steel, plastic and rubber. To expand the range of excitation a steel tube was used. In this case the blow duration reached $\tau \approx 0.2$ msec, and the power range could change within the limits of 500 to 5000 N. A signal from the power generator was sent to the charge amplifier of model 2635, which allows measurings to be performed at low frequencies, starting with 0.2 Hz or 2 Hz.

For measuring of the tube wall vibration an accelerometer 4370 was used. The given signal through the charge amplifier 2635 has been recorded on a four-channel tape recorder 7005 simultaneously with the signal, picked off from hammer power generator. Calibration of the velocity generator was carried by means of the calibrating vibrator 4294.

Two ways of tube excitation have been used: hammer blows in the middle of the tube from above (at a vertical plane) and from one side (at a horizontal plane). The measuring points were located as shown in Fig. 5.

Measurement data processing was carried out by means of a two-channel signal analyser of real time model 2034. As to its parameters and possibilities, the analyser is an ideal device for experiments, carried out with the use of blow hammer. It allows such negative factors, characteristic of blow measurements, as small ratio of a response signal to noise and overload, to be eliminated.

An optimum signal ratio to noise is ensured with the help of autosetting of input attenuators. Further ratio increase is achieved by the use of window functions: pulsed function is used at the power measuring channel and exponential function at the acceleration measuring channel.

The window functions applied are shown in Fig. 6. On installing the input attenuators of 2034 analyser all signals

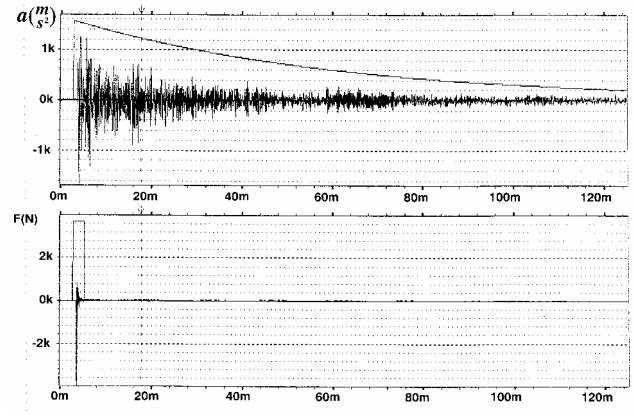

Fig. 6. **The curves of dependence of the magnitude of force *F* (at the bottom) and acceleration *a* (on top) at point 1a**

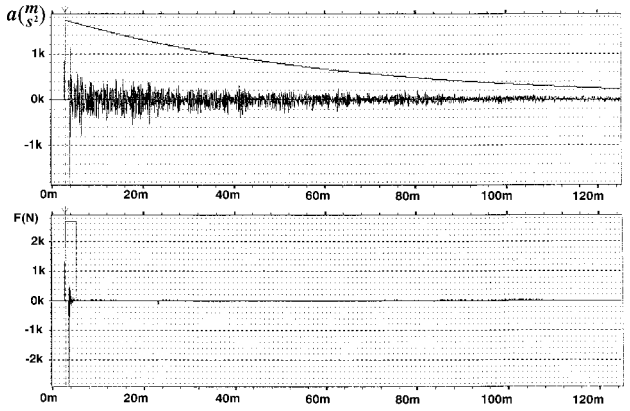

Fig. 7**. The curves of dependence of the magnitude of force *F* (at the bottom) and acceleration *a* (on top) at point 1**

with overload are excluded. In addition, not recorded are signals weak at level. Thus, the analyser makes it possible to select at data processing optimum as to their level values of power and acceleration. As a result the curves of power *F* and of acceleration *a* depending on the time, input impedance Z_e, tube admittance *Y* and eigenspectra *F* and *a* at narrow frequency bands have been obtained.

Measurement results and analysis of the problem under study

The curves of power (at the bottom) and acceleration (on top) dependence on the time at points 1a and 1, accordingly, are shown in Figs 6 and 7. The total record length is 125 msec. Here also are well-seen window functions: pulsed (at the bottom) and exponential (on top).

Narrow band spectra of power (at he bottom) and acceleration (on top) at excitation points 1a and 1, accordingly, are provided in Figs 8 and 9. The analysis band equals 8 Hz. The range of frequency changes is equal to 0-6.4 kHz.

As is seen from figures, the power spectrum is even and it decreases gradually within the range of given frequency. This is defined by the fact that even though the duration of a power impulse is small, it is final. A great

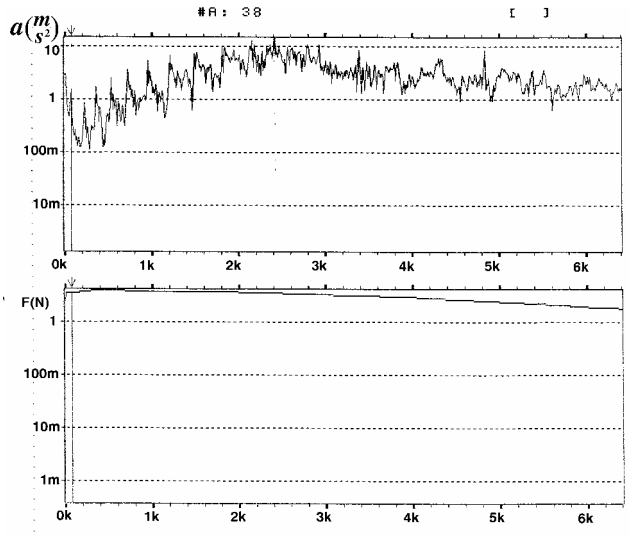

Fig. 8. **Eigenspectrum of force *F* (at the bottom) and acceleration *a* (on top) at point 1a**

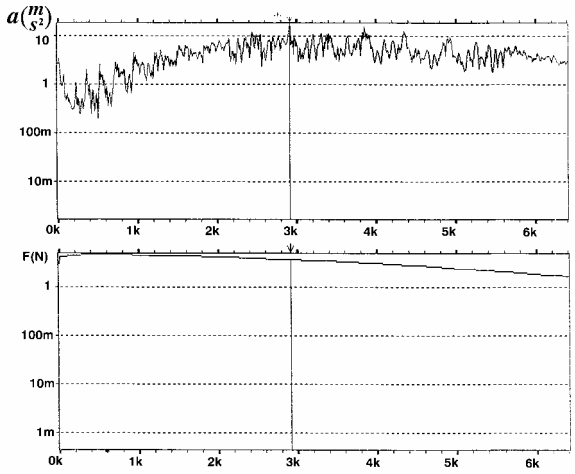

Fig. 9**. Eigenspectrum of force *F* (at the bottom) and acceleration *a* (on top) at point 1**

number of resonances can be seen at the frequency acceleration curve, especially in the range of frequency 0-3 kHz. Maximum spectrum meanings in both cases are located at the medium frequency range where the first longitudinal resonance frequency of the shell $f_l+c_l/2\pi a$ (*a* tube radius, c_l propagation velocity of longitudinal waves in a bar) is placed. In our case f_l=2255 Hz. However, there are some differences. In the case of blow from one side resonances are more sharply expressed. The value of peaks exceeds 20 dB. The zone of the maximum value is located at the frequency range of 2-3 kHz.

The differences observed may be explained, evidently, by the conditions of fixing on the edges. In a vertical direction one end of the tube is suspended on a string, the other one is supported. In a horizontal direction the suspended end of the tube has greater mobility (low resistance to movement) than in a vertical one. In addition, the movement of the second end of the tube in a horizontal direction.

The fact that resonances are observed right up to high frequencies may be explained by insignificant inner loss (steel inner loss coefficient $\eta \sim 10^{-4}$) and slight energy loss by radiation and at the edges.

As far as resonance peaks are concerned, their relation with rotary or longitudinal tube vibrations is hardly probable, since they are weak at excitation and of little importance for radial displacement. Most probably, they are caused by vibrations of such tubes as "beams" ones or by inside radial air resonances.

As is shown in [3], the system of equations of cylindrical shell movement at $n=1$ may be reduced at low frequencies to one equation of flexural vibration movement of the tube.

$$\frac{\partial^2 y}{\partial t^2} + c_n^2 r_0^2 \frac{\partial^4 y}{\partial x^4} - r_0^2 \frac{\partial^4 y}{\partial x^2 \partial t^2} = 0. \qquad (9)$$

where y - displacement of cross-section tube; $r_0 = a/\sqrt{2}$ - its radius of inertia, $c_l = \sqrt{E/\rho}$ - velocity of longitudinal vibrations (in a bar), E and ρ Young's modulus and material density, a tube radius.

It is possible to show that at frequencies lower the frequency of the first longitudinal resonance, $f_l = c_l/2\pi a$, the member, accounting cross-section inertia, may be neglected and written as a wave number of flexural vibrations of the tube (as a beam) in the form

$$k = \sqrt{\frac{\omega}{c_l r 0}}. \qquad (10)$$

In the first approximation a model may be scrutinised as a console with some effective length l_{ef}, disposed between a free part of the tube (6.5 m) and its full length (~9 m). After calculation of number of variants, it was found that a relatively good compliance with the experiment is obtained at l_{ef}=7,5 m. In accordance with [11] resonance frequencies are determined from the equation

$$f_{qp} = \frac{\beta_q \cdot c_n a}{2\sqrt{2}\pi l_{ef}^2}. \qquad (11)$$

The values β_q are given in Table 1.

Table 1.

β_1	β_2	β_3	β_4	β_5	β_6
1,875	4,694	7,855	10,996	14,137	17,279

Calculated according to formula (11) frequencies are provided in Table 2.

Table 2

f_1	f_2	f_3	f_4	f_5	f_6
9	81	227	444	734	1097

Frequencies are determined and are given in Table 3.

Table 3

f_r Hz	8	72	224	360	528	728	952	1208

It is evident from comparing Tables 2 and 3 that first three frequencies and f=728 Hz coincide well with each other. This gives the grounds to affirm that a number of resonance frequencies in the eigenspectrum of wall vibrations are defined by beam vibrations of the tube.

Some resonance frequencies within spectrum may be excited by the inner radial oscillations. For example, at $n=1$ the first resonance frequency f_1=354 Hz, i.e., is located quite close to the measured frequency 360 Hz.

Some frequencies may be defined by tube resonance oscillations at a mode with n=2, since at concentrated

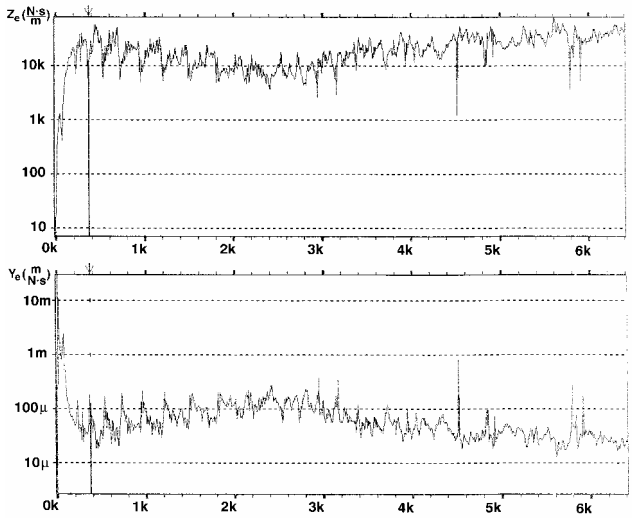

Fig. 11. **Modulus frequency characteristics of input impedance (on top) and admittance (at the bottom) of the tube at excitation at point 1a**

power modes with $n=1$ and 2 are subject to easy excitation.

Tube wall vibration measurements, conducted at different points, show that general character of vibration acceleration changes in the range of given frequency. It has been observed that the further from the point of excitation the lower the resonance peaks. As an example the spectrum of accelerations at p. 2, depicted in Fig. 10, located at a distance of ~1.6 m from the point of excitation.

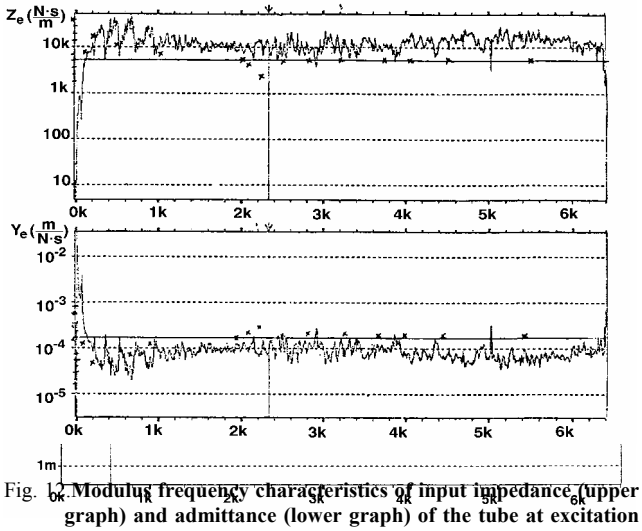

Fig. 12. **Modulus frequency characteristics of input impedance (upper graph) and admittance (lower graph) of the tube at excitation at point 1**

Fig. 10. **Eigenspectrum of the excitation force *F* at point 1 (at the bottom) and acceleration *a* at point 2 (on top)**

The measuring of input admittance *Y* and impedance Z of the tube by concentrated excitation is of great interest. Their frequency characteristics are given in Figs 11 and 12. The curves in Fig. 11 are related to the case of excitation of the tube from aside (p. 1a), the curves in Fig. 12 from above. The same regularity, which is observed in vibration spectra, is noted once again. At excitation from above in a vertical plane the curve *Z* (the upper graph in Fig. 12) almost does not change at all frequencies, on the average. Its value is located in the region 10^4-$2\cdot10^4$ kHz/sec. The most pronounced resonances are placed in the area of frequency up to 1 kHz. At excitation from aside the spread of the value Z in relation to the mean value is significantly higher. For better understanding of the results obtained calculations of input admittance Y_e and impedance Z_e of infinite cylindrical shell at concentrated excitation have been conducted. The algorithm, given a detail study by M. Heckl and D.Gužas [1,2], was taken as a basis of calculation. In accordance with it admittance Y_e may be written in the form

$$Y_e = \sum_{n=0}^{\infty} Y_n, \qquad (12)$$

where n - azimuthal number N. $Y_n = \sum^{4} Y(k_j)$ and k_j - dispersive equation roots located at the upper half-plane of complex values k. Summing up according to azimuthal numbers N was limited by values $|N_0|$, when $|N_0|\varepsilon\left|\sum_{n=0}^{N_0} Y_n\right|$. While calculating, the given accuracy was ε=0.01.

Calculation results are given in Figs 11 and 12. The graphs show that at low frequency range from 100 to 1000 Hz calculated values of input impedance $|Z_e|$ modulus are located within the limits of the experimental dimensions obtained. Later impedance $|Z_e|$ decreases within the frequency range of longitudinal resonance f_l=2255 Hz, where the length of one longitudinal wave may be located into the circumference and later a constant quantity $Z\approx=6\cdot10^3$ (kgs/cm) is obtained.

It should be noted that input impedance of infinite plate at concentrated excitation is equal $Z_p = 8\sqrt{Bm} = 2.31\rho_m c_0 h^2$, where B and m - flexural rigidity and linear density of a plate, c_0 - velocity of longitudinal waves. For the plate of which the shell is made Z_p=6,17·10^3 (kg/s), i.e., it coincides with value $|Z_e|$ at frequencies higher than f_l.

A comparison of an experiment with the theory at frequencies $f>f_l$ show that measured meanings $|Z_e|$ are located somewhat higher than calculated ones (see Fig. 12).

Conclusions

1. Complex impedances for acoustic estimates of radiators of vibration fields were found.

2. Methods for calculation of these impedances for thin-walled constructions were presented.

3. The experimental installation created gave the possibility to investigate the character of vibration and propagation along the experimental tube. At concentrated excitation also to define its input impedance and admittance in the narrow bands of frequencies.

4. In the installation using an analyser 2034, the possibility was created at experimental data processing to select optimum as to their level values of power and acceleration, as well as those of impedance and admittance ant their dependence on time.

5. The power spectrum is even and it decreases gradually with the frequency, since the duration of a power impulse is small, it is final.

6. A great number of resonances can be seen at the acceleration spectrum, and, moreover, maximum spectrum meanings are located at the medium frequency range where the first longitudinal resonance frequency of the shell is placed.

7. The propagation of resonance up to high frequencies may be explained by insignificant inner loss of a steel tube and slight energy loss by radiation and the edges.

8. Some resonance frequencies within spectrum may be excited by the inner radial oscillations.

9. The further from the point of excitation the lower the peaks of resonance.

10. The results of measurings of input impedances and admittances of the tube showed that the same regularity is observed also in vibration spectra.

The most pronounced resonances are placed in the area of frequency up to 1 kHz.

11. A comparison of an experiment with the theory showed that measured meanings of impedance are located somewhat higher than calculated ones. Therefore for determining of impedances and admittances the given methods of calculation may be used.

References

1. **M. Heckl.** Vibrations of Point-Driven Cylindrical Shell // J.Acoustical Society of America. 1962. Vol. 34, No. 10. P.1553-1557.
2. **A. Cummings.** Higher Order Mode Acoustic Transmission Through the Walls of Rectangular Ducts // Journal of Sound and Vibration. 1983. No. 90. P. 193-209.
3. **A. A. Kornecki.** Note on Beam-Type Vibrations of Circular Cylindrical Shells // Journal of Sound and Vibration. 1971. No. 14(1). P.1-6.
4. **D. Gužas.** Normal impedance of Thin-Walled Cylindrical Shell // Vibration Engineering. 1987. Vol. 1. P. 133-140.
5. **A. Filippov.** Oscilations of Deformed Systems. Moscow: Mashinostroenie, 1970. P. 734. (In Russian)
6. **L. Landau, E. Lifshits.** The Theory of Elasticity. Moscow: Nauka, 1987. P. 734. (In Russian)
7. **Baron Rayleigh.** The Theory of Sound. Moscow, 1955. P. 503. (In Russian)
8. **L. Borisov, D. Gužas.** Sound Insulation in Machine-Building. Moscow: Mashinostroenie, 1990. P. 256. (In Russian)
9. **Yu. Konenkov, M. Davtyan.** Random Mechanical Processes in the Equipment of Machines. Moscow: Mashinostroenie, 1988. P. 272. (In Russian)
10. **D. Gužas.** The Excitation of Oscillations of a Cylindrical Shell By Concentrated Efforts // Vibrotechnika. 1988. No. 4(61). P.44-49.
11. **S. P. Timoshenko.** Oscillation in the Field of Engineering. Moscow, 1967. P. 444. (In Russian)

D. Gužas

Cilindrinio kevalo modelio dinaminių charakteristikų teoriniai ir eksperimentiniai tyrimai

Reziumė

Darbo tikslas - supaprastinti cilindrinių kevalų ir analoginių elementų teorinius tyrinėjimus virpesių ir garso perdavimo bei jų izoliacijos uždaviniams spręsti. Šiame darbe, taikant modelius, tiriama virpesių sužadinimo sutelkta jėga, pobūdis ir jų sklidimas vamzdžiais bei cilindriniais paviršiais.

Daug dėmesio skiriama įėjimo impedanso ir admitanso tyrimui, esant sutelktam sužadinimui mažame dažnių diapazone. Tyrimų rezultatai pateikti grafikuose. Eksperimentinių tyrimų rezultatai gerai sutampa su teorinių impedanso nustatymo metodų rezultatais, pateiktais autoriaus darbuose [4, 8].

DOI: 10.5755/j01.u.30.2.7896